

Photonic Reservoir Computing for Nonlinear Equalization of 64-QAM Signals with a Kramers-Kronig Receiver

Sarah Masaad⁽¹⁾, Emmanuel Gooskens⁽¹⁾, Stijn Sackesyn⁽¹⁾, Joni Dambre⁽²⁾, Peter Bienstman⁽¹⁾

⁽¹⁾ Photonics Research Group, Department of Information Technology, Ghent University – imec, Belgium
sarah.masaad@ugent.be

⁽²⁾ IDLab, Department of Information Technology, Ghent University - imec, Belgium

Abstract *Photonic reservoir computing is a promising processing solution for the equalization of fiber optic communication signals. We simulate the nonlinear equalization of 64 Quadrature-Amplitude Modulated signals using a fully passive space multiplexed reservoir. The system deploys direct detection using the recently proposed Kramers-Kronig receiver. ©2022 The Author(s)*

Introduction

The ever-increasing demand for data traffic requires challenging current limitations in both transmission and processing technologies. As processing distorted signals is often required after transmission, the throughput and complexity of the system is largely impacted by the digital signal processing (DSP) deployed.

Advances in photonics enabled shifting focus to optically implementable processing solutions. Indeed, the maturing field of optics boasts several features that make it useful in aiding or replacing digital signal equalization. This includes high bandwidths, deployment as integrated circuits, and parallelism by wavelength multiplexing.

An example of optical processing is the photonic reservoir computing [1–3]. A reservoir can be created from a dynamic system by defining function-performing *nodes* that leverage the system's natural nonlinearities. The nodes are connected through weighted *connections* that are tolerant to the inherent manufacturing variations or natural uncertainty present in hardware. These physical reservoirs are then leveraged for performing a range of tasks in machine learning. Of particular interest is the nonlinear equalization of signals, which is a demanding problem for legacy DSP resulting in high latency and power consumption. We attempt to address this issue in coherent optical communication systems that use Quadrature-Amplitude Modulation (QAM). To simplify the detection process, which is otherwise hardware-demanding, the recently proposed Kramers-Kronig (KK) receiver [4] is used. The KK receiver boasts a simple hardware implementation consisting of a single photodiode, and performs the phase reconstruction of the complex signal by leveraging the well-known KK relations. This receiver has been gaining popularity due to its hardware simplicity and accurate signal reconstruction compared to other schemes [5,6]. An important system consideration is that a high-

power subcarrier must be added to the signal either at the receiver or the transmitter. For complexity and cost constraints, the latter is preferred but would give rise to high nonlinear effects in the transmission fiber.

To this end, we numerically simulate the use of a passive photonic reservoir for the nonlinear equalization of a high intensity 64-QAM signal propagating in a Standard Single Mode Fiber (SSMF) spanning lengths of up to 100 km and received by a KK receiver. Nonlinearities originating from the fiber Kerr effects and the transmitter's nonlinear behavior are considered. In contrast to classical RC which is trained using ridge regression, our equalizer backpropagates through the entire receiver and post-processing algorithm to train 16 complex readout weights in the optical domain. As we will show, this provides additional nonlinearity and better performance. Testing errors reported fall well below $1e^{-3}$ pre-Forward Error Correction (FEC) Bit Error Rate (BER). This passive, latency free, and symbol rate insensitive implementation is a powerful solution for mitigating communication system errors, which along with the KK receiver can be viable solutions for the deployment of high data rate and high modulation format systems for inter- and intra-data center applications.

Photonic Reservoir

Our implementation of the reservoir is a Silicon Nitride based photonic integrated circuit, making it a small-footprint, on-chip reservoir. This reservoir, which we term the Four-Port Architecture [7], is made of 3x3 Multi-Mode Interferometers (MMI) that serve as nodes and are interconnected by waveguides. Every node has an external input, an external output, two inputs from within the reservoir, and two outputs leading into the reservoir. External inputs are used for injecting signals into the reservoir and external outputs are connected to weighting elements where they can be weighted and

summed. The waveguide delay lines connecting nodes slow down the signal to allow meaningful mixing on the timescales of the input signal. A 16 node reservoir is shown in Fig 1.

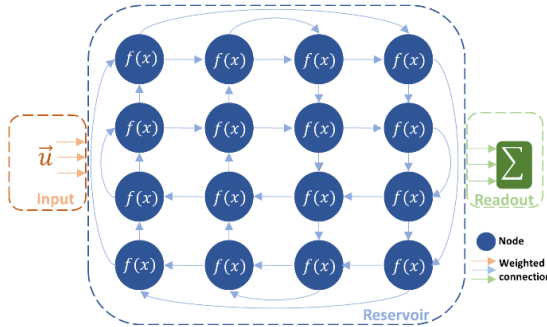


Fig. 1: 16 node MMI based reservoir.

The waveguide-induced phase and amplitude changes that occur in the reservoir are largely caused by the manufacturing tolerances and imperfections inevitably present in silicon photonics. These act as internal reservoir weights that we do not train or optimize. We are, however, interested in the length of these lines, as they control the amount of memory in the reservoir and the time differences between two mixing signals. Thus, the delay line length is an optimizable parameter in our setup.

This is a passive reservoir by design; it is driven by the input signal and uses no additional power. Although this is a power advantage, MMIs perform linear functions that just redistribute portions of the inputs over the outputs, which would not be sufficient to solve nonlinear tasks. The required nonlinear transformation is then added through utilizing innate components in the system where the reservoir is inserted and which may be application specific. In a communication system, a receiver performing the squaring function is a suitable candidate [8]. Our system is therefore a variant of a standard reservoir, where the nonlinearity happens after the readout weights as opposed to within the reservoir.

Kramers-Kronig Receiver

The Kramers-Kronig receiver employs a simple photodetector to detect a complex signal's power and reconstructs its complex nature through a series of processing steps. This is possible when a complex signal's phase is uniquely related to its amplitude, which can be guaranteed provided that a pair of conditions is respected [9]. First, it

must be a Single Side-Band (SSB) signal. Thus, an additional optical subcarrier should be added to either edge of the signal's spectrum. Second, the subcarrier must have sufficiently higher power with respect to the signal, this is termed the Carrier-Signal Power Ratio (CSPR). In our simulations, error-free reconstruction was achieved at a CSPR around 9 dB.

The KK receiver's pipeline is shown in Fig. 2. Consider a complex signal $s(t)$ that is impinging on a photodetector. The current from the detector, $i(t)$, is the measurable signal obtained and its square root corresponds to $|s(t)|$. Through the receiver operation detailed in [9–11], the complex signal $s(t)$ can be reconstructed from the measured current signal. The nonlinear operations in this pipeline are also leveraged to improve the reservoir's nonlinearity equalization.

System Details and Results

The transmission system is simulated using VPI Photonics TransmissionMaker software [12], where a single polarization 64 QAM transmitter transmits over fiber lengths ranging from 20 to 100 km. The role of the reservoir is to target nonlinearity-induced errors generated from self-phase modulation due to the Kerr effect and from the nonlinear response of the modulator. To focus on that role, we compensate linear dispersion separately using a dispersion compensating fiber with matched dispersion parameters to those of the transmission fiber. For pronounced nonlinearities we also transmit the signal at 3 dBm with CSPR of 11 dB. The signal is then amplified to correct for the fiber attenuation and an additional 15 dB of power is added. The receiver is the KK receiver pipeline described in the previous section, where the detector simulated exhibits shot and thermal noise. No other impairments e.g. laser phase noise and polarization mode dispersion are considered. The system setup is shown in Fig. 3.

Simulation of a 16-node reservoir, whose topography is shown in Fig. 1, is done in Photontorch [13]. All the reservoir nodes are connected to the readout and the complex-valued optical weights are trained to approximate the target signal. Initially, the target before the KK receiver is used. This method where the pre-receiver target is used is referred to as the Linear RC (L-RC), in reference to the linear nature of the



Fig. 2: Operations – FFT: Fast Fourier Transform; ln: natural logarithm; KK: KK relations; IFFT: Inverse Fast Fourier Transform; exp: exponential; C.R: Carrier Removal; F.S: Frequency Shift; RRC: Root-Raised Cosine Filter. Signals – $i(t)$: current; F_n^r : frequency coefficients of real signal ($|s(t)|$); F_n^i : frequency coefficients of the imaginary signal $j\varphi(t)$; $s(t)$: complex signal

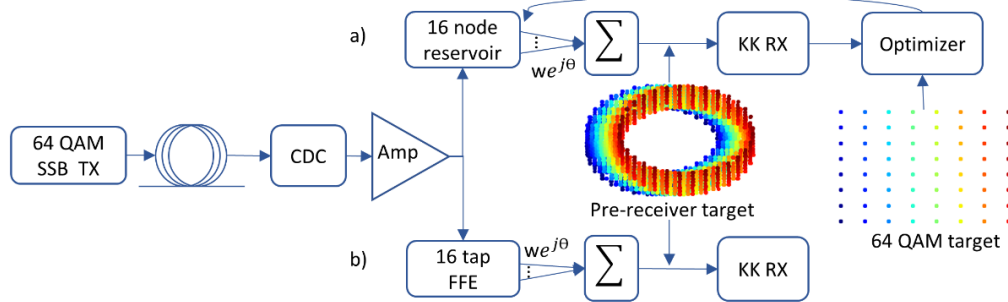


Fig. 3: Simulation setup for 64-QAM signals in SSMF that are dispersion compensated. Nonlinear equalization in: a) 16 node reservoir with complex readout weights found linearly and through backpropagation; or b) 16 tap feed forward equalizer with complex weights found linearly. Acronyms - SSB Tx: Single-sideband Transmitter; CDC: Chromatic Dispersion Compensation; Amp: Amplifier; KK RX: Kramers-Kronig Receiver; $we^{j\theta}$: complex weight with amplitude w and phase θ

readout. The actual target is only available after the KK receiver, thus requiring backpropagation through the receiver blocks to bridge the gap between the readout weights and the final target. This also gives rise to a nonlinear “function” which encompasses the photodiode, the KK algorithm, and the post-processing steps. This is referred to as the Non-Linear RC (NL-RC) since a nonlinear function is now involved. In spite of more complicated training, significant error reduction is obtained through this adjustment as shown in Fig 4. We compare our results to a linear baseline, whose pipeline is shown in Fig 3b, utilizing a 16-tap Feed-Forward Equalizer (FFE) instead of the reservoir. The FFE passes the signal through a series of 15 cascaded time delays. The signals at the output of every delay element and a portion of the original signal are weighted with trainable complex-valued weights and then summed. This is a linear block and would use the target before the receiver for adjusting the weights.

The training dataset is used to find the readout weights as well as to optimize the RC and FFE architectures. For both setups, the length of the delay lines is an optimizable parameter. Sweeps of this value are done independently for every fiber link length and the optimum values are chosen. Optimization sweeps indicate that a time delay of around half the symbol period is optimum for almost all the links studied. The testing dataset, used to investigate the performance of the equalizers, was generated through a Wichmann-Hill generator [14]. Over 130,000 symbols are tested and the statistical BER is found using a gaussian approximation. The subcarrier induces considerable nonlinearities to which the high-level modulation format becomes very susceptible resulting in a BER on the order of $1e^{-2}$. Fig. 4 shows the statistical BER on the test set for the different fiber lengths. Although the distortion is caused by nonlinear effects, the signal benefits from utilizing information from its

neighboring symbols and the BER improves even when using linear schemes, i.e. FFE and L-RC. However, mixing in the reservoir does not directly have a positive impact as compared to that of the FFE. It is only when the nonlinear readout is involved that the BER improves and is on average one third that of the FFE. The NL-RC over all the fiber lengths reduced the BER well below $1e^{-3}$ and maintained this performance with different reservoir simulations and datasets, as indicated by the error bars.

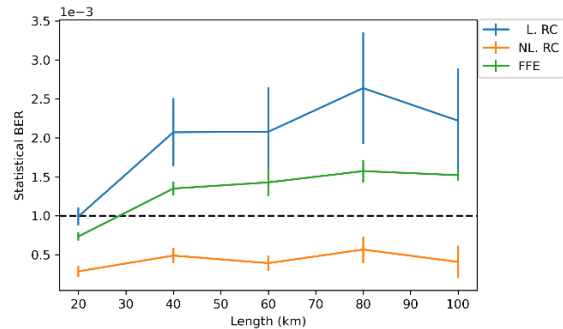


Fig. 4: Testing BER (statistical assuming Gaussian distribution) vs link length for Linear Reservoir (blue) with no external nonlinearity, Nonlinear Reservoir (orange) where the KK receiver is leveraged as a nonlinear block, and an optical

Conclusions

The transmission of a 64 QAM signal and its detection using the KK receiver was numerically shown to benefit from the use of a photonic reservoir to mitigate effects of fiber nonlinearities and transmitter imperfections, surpassing the performance of an optical feed forward equalizer. We used a novel training scheme which included the entire KK processing pipeline to increase the nonlinear computational capacity of the setup. This optical solution is passive, latency free, and insensitive to the signal baud rate.

Acknowledgements

Parts of this work were performed in the context of the EU projects ITN Postdigital (GA860360), Nebula (871658) and Neoteric (GA871330).

References

- [1] G. Van Der Sande, D. Brunner, and M. C. Soriano, "Advances in photonic reservoir computing," *Nanophotonics*, vol. 6, no.3, pp. 561–576, 2017, DOI [10.1515/nanoph-2016-0132](https://doi.org/10.1515/nanoph-2016-0132).
- [2] L. De Marinis, M. Cococcioni, P. Castoldi, and N. Andriolli, "Photonic Neural Networks: A Survey," *IEEE Access*, vol. 7, pp. 175827–175841, 2019, DOI [10.1109/ACCESS.2019.2957245](https://doi.org/10.1109/ACCESS.2019.2957245).
- [3] A. Luginan, A. Katumba, F. Laporte, M. Freiberger, S. Sackesyn, C. Ma, E. Gooskens, J. Dambre, and P. Bienstman, "Photonic neuromorphic information processing and reservoir computing," *APL Photonics*, vol. 5, no. 2, 2020, DOI [10.1063/1.5129762](https://doi.org/10.1063/1.5129762).
- [4] A. Mecozzi, C. Antonelli, and M. Shtaif, "Kramers–Kronig coherent receiver," *Optica*, vol. 3, pp. 1220–1227, 2016, DOI [10.1364/OPTICA.3.001220](https://doi.org/10.1364/OPTICA.3.001220).
- [5] Z. Li, M. S. Erkilinc, K. Shi, E. Sillekens, L. Galdino, B. C. Thomsen, P. Bayvel, and R. I. Killey, "SSBI mitigation and the kramers-kronig scheme in single-sideband direct-detection transmission with receiver-based electronic dispersion compensation," *Journal of Lightwave Technology*, vol. 35, no. 10, pp. 1887–1893, 2017, DOI [10.1109/JLT.2017.2684298](https://doi.org/10.1109/JLT.2017.2684298).
- [6] S. T. Le, K. Schuh, R. Dischler, F. Buchali, L. Schmalen, and H. Buelow, "Beyond 400 Gb/s Direct Detection over 80 km for Data Center Interconnect Applications," *Journal of Lightwave Technology*, vol. 38, no. 2, pp. 538–545, 2020, DOI [10.1109/JLT.2019.2941690](https://doi.org/10.1109/JLT.2019.2941690).
- [7] S. Sackesyn, C. Ma, J. Dambre, and P. Bienstman, "An enhanced architecture for silicon photonic reservoir computing," in *Cognitive Computing - Merging Concepts with Hardware*, 2018, pp. 3–4.
- [8] K. Vandoorne, P. Mechet, T. Van Vaerenbergh, M. Fiers, G. Morthier, D. Verstraeten, B. Schrauwen, J. Dambre, and P. Bienstman, "Experimental demonstration of reservoir computing on a silicon photonics chip," *Nature Communications*, vol. 5, pp. 1–6, 2014, DOI [10.1038/ncomms4541](https://doi.org/10.1038/ncomms4541).
- [9] A. Mecozzi, C. Antonelli, and M. Shtaif, "Kramers–Kronig receivers," *Advances in Optics and Photonics*, vol. 11, no. 3, pp. 480–517, 2019, DOI [10.1364/aop.11.000480](https://doi.org/10.1364/aop.11.000480).
- [10] A. Mecozzi, C. Antonelli, and M. Shtaif, "Kramers-Kronig receivers: supplementary material," *Optical Society of America*, vol. 11, no. 3, pp. 480–517, 2019, DOI [10.1364/AOP.11.000480](https://doi.org/10.1364/AOP.11.000480).
- [11] C. Fullner, M. M. H. Adib, S. Wolf, J. N. Kemal, W. Freude, C. Koos, and S. Randel, "Complexity Analysis of the Kramers–Kronig Receiver," *Journal of Lightwave Technology*, vol. 37, no. 17, pp. 4295–4307, 2019, DOI [10.1109/jlt.2019.2923249](https://doi.org/10.1109/jlt.2019.2923249).
- [12] "VPItransmissionMaker," <https://www.vpi Photonics.com/Tools/OpticalSystems/> accessed on 10 May 2022.
- [13] F. Laporte, J. Dambre, and P. Bienstman, "Highly parallel simulation and optimization of photonic circuits in time and frequency domain based on the deep-learning framework PyTorch," *Scientific Reports*, vol. 9, pp. 1–9, 2019, DOI [10.1038/s41598-019-42408-2](https://doi.org/10.1038/s41598-019-42408-2).
- [14] B. A. Wichmann and I. D. Hill, "Algorithm AS 183: An Efficient and Portable Pseudo-Random Number Generator," *Journal of the Royal Statistical Society. Series C (Applied Statistics)*, vol. 31, no. 2, pp. 188–190, 1982, DOI [10.2307/2347988](https://doi.org/10.2307/2347988).